Journal Pre-proof

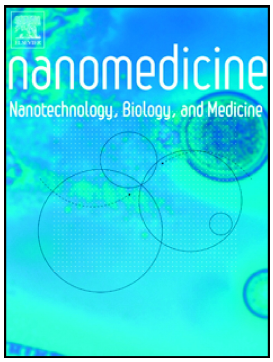

Cell membrane-encapsulated magnetic nanoparticles for enhancing natural killer cell-mediated Cancer immunotherapy

Dan Wu, Xin Shou, Yalan Zhang, Zihan Li, Guohua Wu, Di Wu, Jianguo Wu, Shengyu Shi, Shuqi Wang

PII: S1549-9634(20)30187-8

DOI: https://doi.org/10.1016/j.nano.2020.102333

Reference: NANO 102333

To appear in: *Nanomedicine: Nanotechnology, Biology, and Medicine*

Revised date: 1 October 2020

Please cite this article as: D. Wu, X. Shou, Y. Zhang, et al., Cell membrane-encapsulated magnetic nanoparticles for enhancing natural killer cell-mediated Cancer immunotherapy, *Nanomedicine: Nanotechnology, Biology, and Medicine* (2020), https://doi.org/10.1016/j.nano.2020.102333

Cell Membrane-encapsulated Magnetic Nanoparticles for Enhancing Natural Killer Cell-Mediated Cancer Immunotherapy

Dan Wu[a, b], Xin Shou[c, e], Yalan Zhang[d], Zihan Li[a, b], Guohua Wu[a, b], Di Wu[a, b], Jianguo Wu[a, b], Shengyu Shi[a, b], Shuqi Wang[a, b,*]

[a] *State Key Laboratory for Diagnosis and Treatment of Infectious Diseases, National Clinical Research Center for Infectious Diseases, Collaborative Innovation Center for Diagnosis and Treatment of Infectious Diseases, The First Affiliated Hospital, College of Medicine, Zhejiang University, Hangzhou, Zhejiang Province, 310003, China.*

[b] *Institute for Translational Medicine, Zhejiang University, Hangzhou, Zhejiang Province, 310029, China*

[c] *Guangdong Key Laboratory for Biomedical Measurements and Ultrasound Imaging, Department of Biomedical Engineering, School of Medicine, Shenzhen University, Shenzhen 518000, China;*

[d] *Department of Pharmaceutical Engineering School of Engineering China Pharmaceutical University Nanjing 211198, China*

[e] *State Key Laboratory of Bioelectronics, School of Biological Science and Medical Engineering, Southeast University, Nanjing, Jiangsu 210096, China.*

Statement of funding:

This work was supported by the National Natural Science Foundation of China (31871016), the National Key Research and Development Program (2016YFC1101302) and National Major Science and Technology Projects (2018ZX10732401-003-007) from the Ministry of Science and Technology of China, the National Key Scientific Instrument and Equipment Development Projects (61827806) from the National Natural Science Foundation of China, and the Key Research and Development Program (2019C03029) from the Science and Technology Department of Zhejiang Province.

The authors declare no potential conflicts of interest

Corresponding author at: *State Key Laboratory for Diagnosis and Treatment of Infectious Diseases, National Clinical Research Center for Infectious Diseases, Collaborative Innovation Center for Diagnosis and Treatment of Infectious Diseases, The First Affiliated Hospital, College of Medicine, Zhejiang University, Hangzhou, Zhejiang Province, 310003, China.*

E-mail addresses: shuqi@zju.edu.cn, (Shuqi Wang)

Word count for Abstract: 146
Word count for manuscript: 3982
Number of References: 40
Number of figures: 6
Number of tables: 0
Number of Supplementary online-only files, if any: 1

Abstract

Natural killer (NK) cells have exhibited therapeutic potential for various malignant tumors. However, the cytotoxic effect of NK cells is relatively weak and less specific compared to other immunotherapy approaches such as chimeric antigen receptor T-Cell (CART) therapy, consituting a great challenge for adoptive immunotherapy. Here, we report cell membrane-encapsulated magnetic nanoparticles for activating NK cells and enhancing anti-tumor effects. Magnetic nanoparticles were coated with silicon dioxide (SiO_2), and cancer cell membranes were mixed with Fe_3O_4@SiO_2 to construct cancer cell membrane coated Fe_3O_4@SiO_2 magnetic nanoparticles (CMNPs). The functionalized nanoparticles bearing cancer-specific antigens on the surface effectively stimulated NK cells by enhancing expression of surface activating receptors and boosting anti-tumor function through the secretion of soluble cytotoxic effectors. To conclude, the biomimetic magnetic nanoparticles offer a versatile and powerful tool to present tumor-specific antigens, priming anti-tumor capability, which is promising to enhance NK cell-based adoptive cancer immunotherapy.

Key words: Biomimetic; Magnetic nanoparticles; Cellular membrane; Immunotherapy; Natural killer cells

Introduction

Cancer immunotherapy aims to achieve efficient tumor killing by stimulating the body's own immune system[1-3]. Recently, a number of emerging cancer immunotherapy strategies including monoclonal antibodies (mAbs) [4, 5], immune checkpoint blockade [6-8], adoptive cellular therapy [9, 10] and cancer vaccines [11, 12] have revolutionized traditional cancer treatment and achieved encouraging clinical outcomes. Of them, adoptive cellular therapy is a promising approach whereby autologous immune cells are isolated and activated prior to infusing back into patients to directly kill tumors or to stimulate the host's tumor-specific immune responses. Recently, the efficacy of natural killer (NK) cell-based adoptive immunotherapy has been reported in a number of solid tumors and hematological malignancies, showing great therapeutic potential in cancer treatments [13-16]. Upon binding target cells, NK cells present up-regulated expression of surface activating receptors (*i.e.*, NKG2D, NKp30, NKp44, and NKp46) for tumor killing [17, 18]. Alternatively, NK cells can interact with the fragments of immunoglobulin G1 (IgG1) through FcγRIIIa (CD16) for antibody-dependent cellular cytotoxicity (ADCC) mediated tumor killing [19]. NK cells derived soluble factors such as granzyme B and perforin can also be directly involved in tumor killing [20]. Within larger immune response cascades, NK cells can possess immunomodulatory effects through recruiting T lymphocytes to participate in the adaptive immune responses by secreting IFN-γ, IL-2, *etc* [21]. Importantly NK cells, as opposed to T lymphocytes, do not induce graft-versus-host disease (GVHD) owing to immune compatibility [22, 23], making them suitable for a wide range of autologous and allogenic contexts. However, the proportion of human NK cells is low (i.e., approximately 5-7% of lymphocytes) in peripheral blood, and they are generally in a dormant/silent state, meaning they cannot meet the current clinical demand for therapeutic applications.

Currently, the NK cell-based adoptive immunotherapy requires the isolation of NK cells from the peripheral blood a patient or a healthy donor, followed by *in vitro* activation and expansion, and then infusion to the patient for oncotherapeutic effects [22, 24-26]. This strategy is highly dependent on co-culturing of artificial antigen-presenting cells (4-1BBL-mIL-21-K562 cells) capable of stimulating trans-membrane IL-21 on NK cells [25, 27]. Though effective, this approach still suffers from the disadvantages due to the presence of the residual feeder cells and long expansion time, limiting the clinical application of NK cell-based adoptive immunotherapy. In workarounds, strategies such as NK cell-encapsulated porous microspheres have been employed as more targeted approaches that can decrease the amount of NK cells needed, whereby direct injection in tumor sites can inhibit the growth of tumor cells and prevent tumor recurrence [23]. Nevertheless, the functionality of NK cells needs to stimulated for enhanced treatment outcomes. As such, biomimetic engineering nanoreactors using cancer cell membranes has been widely used for functional mimicking [28, 29]. For instance, Cao *et al*., reported drug-delivery liposomes encapsulated by macrophage membranes for targeting metastatic sites of lung cancer [30]. The macrophage membrane was modified to enhance the tumor targeting and cellular uptake of drug-delivery liposomes, promoting the inhibitory effects on cancer metastasis. In another study, Fang *et al*., used cancer cell membranes derived from B16-F10 mouse melanoma cells to coat a PLGA core as a means of cancer vaccination [31]. Several recent studies have also reported that cancer cell membrane-encapsulated nanomaterials with tumor-specific antigens can activate dendritic cells (DCs), and present antigens to T cells, inducing T cell-mediated responses against cancer [32-35]. However, the nanoparticle-based antigen-presenting strategy for NK cell activation *in vitro* has not been reported.

Here, we developed an *in vitro* NK cell activation strategy by encapsulating magnetic nanoparticles in tumor cell-derived membrane with embedded tumor-specific antigens for enhanced NK cell-based immunotherapy (**Figure 1**). Magnetic Fe_3O_4 nanoparticles were first modified with a silicon dioxide layer to increase biocompatibility, stability and dispersion, and then encapsulated into HepG2 hepatoma cell-derived cellular membranes, forming cancer cell membrane coated $Fe_3O_4@SiO_2$ magnetic nanoparticles (CMNPs). These nanoparticles upregulated the expression of surface activating receptors and markers on NK cells and subsequently induced the secretion of cytotoxic factors (e.g., perforin and granzyme) for enhancing NK cell-mediated anti-tumor effects against HepG2 cells. Interestingly, the activated NK cells also showed cytotoxicity against A375 melanoma cells. Thus, cell membrane-based biomimetic magnetic nanoparticles, due to enhanced tumor antigen-presentation, hold great potential for cancer adoptive immunotherapy.

Methods

Preparation of superparamagnetic $Fe_3O_4@SiO_2$ core-shell nanoparticles

To synthesize superparamagnetic $Fe_3O_4@SiO_2$ core-shell nanoparticles, we used a hydrothermal method. In brief, 0.26 g $FeCl_3$, 0.40 g PSSMA, 1.20 g NaAc, 60 μL H_2O and 16 mL EG from Sigma-Aldrich (St Louis, USA) were vigorously stirred for about half an hour until the solution became uniformly yellow by using a magnetic stirrer at room temperature. Next, 0.24 g of sodium hydroxide was added to the solution with constant stirring until fully dissolved [36]. Then, the solution was mixed with 20 mL of tetrafluoroethylene in a stainless-steel autoclave, with the resulting hydrothermal reaction being regulated at 190 °C for 9 h. After allowing the solution to cool down to an ambient temperature, the Fe_3O_4 nanoparticles were magnetically

separated. Next, a solution of ethanol and water at a ratio of 1:1 was used to disperse and wash the magnetically separated Fe_3O_4 nanoparticles three times, and was finally dispersed in H_2O. The SiO_2 shell was capped on Fe_3O_4 nanoparticles by a modified Stöber method [36]. An aqueous solution containing Fe_3O_4 nanoparticles was added to 2 mL of ammonium hydroxide and 40 mL of ethanol, followed by 5 minutes of sonification. The solution was then deposited in a 25 mL three necked flask submerged in water at 50 °C, and then was stirred at 600 rpm for 10 min. The mixture was continuously stirred for 1 h, and every 20 min, 20 μL of tetraethyl orthosilicate (TEOS) was added. Finally, the Fe_3O_4@SiO_2 nanoparticles were magnetically separated, and rinsed three times with a 1:1 ethanol and water mixture before being finally dispersed in water.

Preparation and characterization of CMNPs

To synthesize the CMNPs, cancer cell membrane was separated following the instructions of Membrane and Cytoplasmic Protein Extraction kit (Sangon Biotech, Shanghai). The cancer cells were lysed and the cell suspension was immediately undergone through a repeated freezing and thawing cycle in liquid nitrogen for 6 times [33]. Then, the cell pellet was removed *via* centrifugation for 10 min at 4100 rpm. The resulting supernatant containing the cytoplasm and membrane was centrifugated at 18,000 rpm for 1 h in order to isolate them. The cancer cell membranes were washed by rinsing once with cool 1× PBS once and spun down at 14,800 rpm for 10 min. The membrane pellet was resuspended in 1×PBS and mixed with Fe_3O_4@SiO_2 core-shell nanoparticles, and then was filtered *via* a 400 nm pore size polycarbonate membrane by a HandExtruder (Genizer LLC, California, USA). Then, the mixture was spun again at 14,800 rpm for 20 min to collect the CMNPs in the pellet. As a control for future experiments, cancer cell membranes not mixed with the Fe_3O_4@SiO_2 core-shell nanoparticles were passed through

the polycarbonate membrane with a pore size of 400 nm as well. Finally, the CMNPs and cancer cell membranes were stored in 1 × PBS solution at 4 °C. The nanostructures of the Fe_3O_4, Fe_3O_4@SiO_2 nanoparticles and CMNPs were assessed using transmission electron microscopy (TEM) (JEOL, JEM-2100). No staining was used while imaging with TEM. A Zetasizer Nano instrument (Malvern Instruments, Worcestshire, UK) was used to determine the hydrodynamic dimensions and ζ-potentials of Fe_3O_4, Fe_3O_4@SiO_2, CMNPs and cancer cell membrane vesicles. For detecting the encapsulation efficiency of cancer cell membrane coating on the surface of Fe_3O_4@SiO_2 nanoparticles was calculated by the below formula:

Encapsulation efficiency (%) = m_{total}-m_{free}/m_{total} ×100%

Where m_{total} refers to total mass of cancer cell membrane proteins, and m_{free} is the mass of cancer cell membrane proteins in the supernatant.

Characterization of tumor-associated antigens on CMNPs

SDS-PAGE electrophoresis was conducted to evaluate the profile of protein expression in the cancer cell lysate, CMNPs, and cancer cell membranes. A Membrane and Cytoplasmic Protein Extraction kit was used to separate the membrane proteins from the cancer cell membrane and CMNPs, which was further characterized using gel electrophoresis. A uniform protein concentration was used for all samples, and Coomassie Blue was used for staining. Cancer cell cytosol was performed as a control. Moreover, tumor-specific membrane protein epidermal growth factor receptor (EGFR) was detected by western blotting with uniform protein concentration in all samples. In the western blot, following the electrophoresis on a 10% SDS-polyacrylamide gel, samples were moved onto polyvinylidene fluoride (PVDF) membranes (Millipore, Bedford, MA, USA). Each sample was then treated with primary EGFR-Specific

Rabbit Polyclonal antibody and β-actin antibody (Proteintech, Chicago IL, USA), followed with HRP-conjugated Affinipure Rabbit Anti-Goat IgG (H+L). The protein signals were measured with ChemiDoc MP Imaging System (Bio-Rad, CA, USA). β-actin protein signals were also observed as a loading control. In addition, the expression of membrane-specific MHC class I chain-associated molecules A/B (MICA/MICB) in CMNPs was detected by flow cytometry. CMNPs were briefly incubated with PE anti-human MICA/MICB antibody (Biolegend, San Diego, CA) for half an hour at 4 ℃ and then detected by the FACS Calibur system (BD Biosciences).

Isolation of NK cells from peripheral blood

Peripheral blood mononuclear cells (PBMCs) were isolated from venous blood of healthy donors by density gradient centrifugation. purified NK cells were then isolated from PBMCs following the instructions of NK Cell Isolation Kit (Miltenyi Biotec, Germany). First, we prepared single cell suspensions and determined the number of cells. Simultaneously, we prepared a PBS solution (pH = 7.2) consisting of 2 mM EDTA and 0.5% BSA. Then, we added 10 μL of NK cell biotin-antibody for every 10^7 cells, and incubated at 4 ℃ for 5 min. Next, we added 30 μL separation buffer to 20 μL of NK cell MicroBead cocktail (Miltenyi Biotec, Germany) to 10^7 cells, which was then mixed well and incubated at 4 ℃ for 10 min. Finally, NK cells were automatically separated using autoMACS® Pro Separator (Miltenyi Biotec, Germany).

Biocompatibility of Fe_3O_4@SiO_2 nanoparticles

The biocompatibility of Fe_3O_4@SiO_2 nanoparticles with NK cells was evaluated using Cell Counting Kit 8 (CCK8) (Dojindo, Kumamoto, Japan). NK cells (8×10^4/mL) were seeded into

each well of a 96-microwell plate for 100 μL and co-cultured with 0, 25, 50, 100, 250, and 500 μg/mL of Fe_3O_4@SiO_2 for 24 h. Then, the cell viabilities were measured in accordance with the instructions from the manufacturer. The CCK-8 working reagent (1/10 volume of culture medium) was pipetted into each well and then maintained with 5% CO_2 concentrations at 37 °C for 3 h. Finally, a plate reader (Synergy™ HTX) was utilized to measure the absorbance at 450 nm.

Characterization of activated NK cells stimulated by CMNPs

The cytotoxicity of CMNPs containing various membrane proteins towards NK cells was evaluated similar to the section above. NK cells (8×10^4/mL) were seeded into a 96-microwell plate and co-cultured with CMNPs containing 0, 5, 10, 25, 50, 100, and 250 μg total membrane protein for 24 h. Then, the NK cell viability was measured using CCK8 assay. The protein profile of activated NK cells was characterized using Enzyme linked immunosorbent assay (ELISA) and flow cytometry. First, the NK cells (1×10^5/mL) were exposed to CMNPs containing 0, 5, 10, 25 μg total membrane protein for 12 h, 24 h, and 48 h. Then, to reduce potential prolonged and wanted influence of magnetic CMNPs towards NK cells, CMNPs were removed by a magnet after NK cells were activated. The concentration of granzyme B, IFN-γ and perforin from NK cells were determined using ELISA assay kits (Neobioscience, Shenzhen, China) according to the instructions from the manufacturer. Absorbance measurements were conducted at the wavelength of 450 nm using a plate reader. To facilitate flow cytometry, NK cells were seeded into 24-well plate at the number of 1×10^5/mL and cocultured with CMNPs containing 10 μg total membrane protein for 12 h. After removal of CMNPs, the activated NK cells were rinsed and then resuspended in PBS and cocultured with the following antibodies:

PE-conjugated anti-NKp30 (IgG1, AF29-4D12), anti-NKp44 (IgG2b, 44.189), PE-Cyanine7-conjugated anti-NKG2D (IgG2b, 1D11), and anti-NKp46 (IgG1, 9E2) antibodies from eBioscience (San Diego, USA). FACS Calibur (BD Biosciences). Data analysis was executed using CellQuest Pro software.

In vitro anti-tumor activity testing of activated NK cells

To test the cytotoxicity of the NK cells activated by CMNPs, Calcein-AM staining and lactate dehydrogenase (LDH) release test were utilized. The HepG2 and A375 cells (2×10^5/mL) were pre-labelled with calcein-AM for 15 min, then seeded in 24-well plate and cultured for 24 h. NK cells were first stimulated with CMNPs containing 10 μg total membrane protein for 24 h, then HepG2 and A375 cells were exposed to non-stimulated NK cells or CMNPs-stimulated NK cells for 6 h or 12 h with an effector (E): target (T) ratio of 1: 5, 1:1, or 5:1. Cell staining was carried out using Calcein-AM staining assay kit in conjunction with a Nikon A1 confocal fluorescence microscope to visualize the anti-tumor activity. LDH assay kit (Dojindo, Kumamoto, Japan) was utilized to quantify the tumor killing effect of activated NK cells according to the manufacturer's instructions.

Statistical analysis

Statistical analysis was conducted using the Origin 9.1 software. Data are plotted as mean ± SD. The comparisons between groups were evaluated by one-way analysis of variance (ANOVA) test. A P value ≤ 0.05 was used to indicate statistical significance.

Results

Fabrication and characterization of composite CMNPs

Figure 1 shows the process of preparing CMNPs. First, Fe_3O_4 magnetic nanoparticles were synthesized, and SiO_2 was modified on the surface to construct biocompatible Fe_3O_4@SiO_2 nanoparticles. Results from the scanning electron microscopy (SEM) show the surface topography of Fe_3O_4@SiO_2 and Fe_3O_4 nanoparticles. **Figure S1** shows the diameter of Fe_3O_4@SiO_2 nanoparticle increased, and its surface became smoother after modification with SiO_2. Next, purified cell membrane was isolated from HepG2 cells and mixed with Fe_3O_4@SiO_2 nanoparticles to fabricate functionalized CMNPs. Through protein concentration determination, we found that the encapsulation efficiency of cell membrane on nanoparticles were 70.6% ± 0.54%. The morphology of Fe_3O_4, Fe_3O_4@SiO_2 and CMNPs was characterized by transmission electron microscopy (TEM). **Figure 2, *A*** shows the CMNPs were nearly spherical and had a core-shell structure after cancer cell membrane encapsulation. Dynamic light scattering (DLS) experiments demonstrate that the mean radius of Fe_3O_4@SiO_2 nanoparticle was 210 nm, and the cancer cell membrane were around 230 nm in radius. After coextrusion and centrifugation, **Figure 2, *B*** shows the CMNPs were approximately 220 nm in radius, and the cancer cell membrane layer on the surface of Fe_3O_4@SiO_2 were approximately 10 nm in size. The zeta potential measurement showed that the average surface charge of Fe_3O_4@SiO_2 nanoparticle after SiO_2 coating changed to -38 mv, while the surface charge of final CMNPs was approximately -28 mv (**Figure 2, *C***). Compared with Fe_3O_4@SiO_2 nanoparticle, the size of CMNPs was slightly larger and the surface charge raised to the equivalent level as the cell membrane due to the cancer membrane coating. Taken together, the cancer cell membrane was successfully coated as the outer layer of CMNPs.

Characterization of tumor-associated antigens on CMNPs

To determine whether functionalized membrane proteins were retained on the CMNPs, the protein content of CMNPs was first analyzed by gel electrophoresis. Coomassie staining shows the protein profile of cancer cell membrane and cancer cell lysate, and the protein profile of CMNPs was in accordance with that of cancer cell membrane (**Figure 3, *A***). This further indicates that the cancer cell membrane was successfully coated on the surface during the preparation of CMNPs. Next, to confirm the retaining of tumor-associated antigens on CMNPs, we analyzed the expression of EGFR *via* western blot. **Figure 3, *B*** shows the membrane protein EGFR was observed in cancer cell membrane and CMNPs, while cytoplasmic protein marker β-actin was not detected on the CMNPs, indicating that the cell membrane was specifically isolated and the protein content was retained in the fabrication process of CMNPs. In addition, as the expression of membrane receptors MICA/MICB reflect the sensitivity and anti-tumor responses of NK cells, we then detected the presence of membrane receptor MICA/MICB on CMNPs using flow cytometry. The analysis results display that the level of MICA/MICB on CMNPs with HepG2 cell membrane coating was up to 86.2%, which proved to be feasible for *in vitro* stimulation of NK cells. These results show that cancer cell membrane was successfully purified, and tumor-associated antigens were retained in the synthesis of functionalized CMNPs by coextrusion and centrifugation.

Functional characterization of activated NK cells stimulated by CMNPs

The cytotoxic effects of Fe_3O_4@SiO_2 nanoparticles to NK cells were first detected by the CCK8 assay. **Figure S2** shows Fe_3O_4@SiO_2 exhibited good biocompatibility to NK cells at a concentration below 100 μg/mL. To diminish the effects of Fe_3O_4@SiO_2 nanoparticles on NK

cell growth, 50 μg/mL Fe_3O_4@SiO_2 was selected to fabricate CMNPs with various amounts of membrane protein. To investigate the potential cytotoxic effects of CMNPs, concentrations of membrane protein was varied within the CMNP solutions added to NK cells, and the viability of NK cells cocultured with CMNPs was measured. **Figure S3** shows the CMNPs with high amount of total membrane protein over 25 μg exhibited cytotoxicity to NK cells. Therefore, CMNPs with total membrane protein below 25 μg were used to activated NK cells. To assess the anti-tumor capability of CMNP-stimulated activated NK cells, the concentration of cytokines of NK cells, including granzyme B, IFN-γ and perforin, secreted in the supernatant was measured *via* ELISA. **Figure 4, *A*-*C*** shows that the NK cells stimulated by CMNPs with 10 or 25 μg total membrane protein had markedly elevated secretion of granzyme B, IFN-γ and perforin owing to the activation of NK cells. As tumor-killing ability of NK cells is related to the surface expression levels of activating receptors, flow cytometry was used to detect the expression of surface receptors such as NKG2D, NKp30, NKp44, NKp46 and CD69 on NK cells stimulated by CMNPs. The results of flow cytometry show that the expression of NKG2D, NKp30, NKp44, NKp46 and CD69 on activated NK cells increased after 12 h of culturing with CMNPs containing 10 μg total membrane protein. Therefore, by co-culture with CMNPs with more time, NK cells were activated to secret more cytotoxic factors and possessed enhanced tumor-killing ability.

In vitro killing of tumor cells by CMNPs-stimulated NK cells

To investigate the cytotoxicity of CMNPs-stimulated NK cells, co-culture of HepG2 or A375 cells with non-stimulated NK cells or CMNPs-stimulated NK cells was performed. Calcein-AM staining shows the survival rate of HepG2 (**Figure 5, *A* and *B***) or A375 (**Figure 5,**

C* and *D) cells after co-culturing with non-stimulated NK cells or CMNPs-stimulated NK cells for 12 h. Activated NK cells had significantly more tumor cell killing effects at an effector-to-target (E:T) ratio of 5:1 than the non-stimulated NK cells. In addition, the level of lactate dehydrogenase (LDH) release after 12 h co-culture of HepG2 cells with the unactivated and the CMNP-stimulated NK cells was measured. **Figure 6, *A*** shows that the cytotoxic effects of the unactivated and the CMNP-stimulated NK cells, co-cultured with HepG2 cells for 12 h with 5:1 E:T ratio, were 18.6% and 86.2%, respectively. In addition, when the E:T ratio was 5:1, the level of LDH in the supernatant of culture medium from A375 cells co-cultured for 12 hours with unactivated and CMNP-stimulated NK cells were 20.3% and 89.6%, respectively (**Figure 6, *B***). The results demonstrate that the NK cells activated by CMNPs had stronger killing effects on HepG2 cells and A375 cells than the unactivated NK cells.

Discussion

As the proportion of NK cells in peripheral blood is low, and that their isolation is expensive and time consuming, it is difficult to meet current clinical needs. Adoptive NK cell immunotherapy, although promising, is significantly affected by these limitations since NK cells are extracted from the peripheral blood of healthy volunteers or cancer patients and are activated and proliferated under the stimulation of artificial antigen presenting cells before being infused back to the patient. Currently, this workflow is highly dependent on NK cell stimulation by artificial antigen presenting cells (*i.e.*, 4-1BBL-mbIL21-K562 cells), through surface expressed transmembrane IL-21[25, 27]. Although their stimulation is effective, the method still has limitations due to the risk of K562 cell residues and the unsolved issue of time-consuming NK cell proliferation.

Membrane encapsulation technology has been widely applied in the field of biomedicine[29, 37]. In order to mimic the antigenic stimulation of NK cells *in vitro*, we prepared multifunctional nanoparticles with an antigenic cell membrane coat to activate NK cells. Magnetic nanoparticles coated with silicon dioxide were selected as inorganic carriers to deliver tumor cell membranes. These nanoparticles can be rapidly assembled and separated under the guidance of magnets, as well as decrease the risk of residual stimulator cells in NK cell infusions. The outer layer of our magnetic nanoparticles was coated silicon dioxide to elicit higher colloidal stability and greater biocompatibility. A biomimetic "tumor cell" could then be subsequently prepared by wrapping antigenic tumor cell membranes around these SiO_2-modified magnetic nanoparticle. We demonstrate these CMNPs can potentially play a key role in stimulating NK cell activation, carrying a variety of membrane proteins, such as EGFR and MICA/MICB. NKG2D, an activated receptor on the surface of NK cells, can recognize MICA/MICB protein expressed by tumor cells under stress, thus triggering NK cells to clear tumor cells[38, 39]. We found that MICA/MICB was highly expressed and retained on the tumor cell membranes of CMNPs, suggesting that CMNPs could be used to stimulate NK cells *in vitro*.

NK cells are the first line of innate immunity in the body, functioning in identifying abnormal cells or invading pathogens. The cytotoxic effect of NK cells depends on the number of cells and effective killing activity. The activity of NK cells is regulated by the dynamic balance betwen signals from activated and inhibited surface receptors[40]. During NK cell activation, surface activated receptors such as NKG2D, NKp46, NKp30, and NKp44 provide activation signals that trigger cytotoxic effects and secretion of cytokines. Therefore, when NK cells are in the activated state, the expression of activated receptors on the cell surface and the level of secreted cytokines will be increased, which aligns with our results demonstrating that

CMNPs can effectively activate NK cells. Compared with unstimulated NK cells, CMNP-stimulated NK cells showed upregulated expression of activated receptors and increased secretion of killing cytokines. Furthermore, we evaluated the anti-tumor capacity of NK cells activated by CMNPs *in vitro*, demonstrating that the activated NK cells had significant tumor killing activity.

Reporting biomimetic cancer cell membrane-encapsulated magnetic nanoparticles for activating NK cells *in vitro*, we propose that the cancer cell membrane coated on CMNPs serves a promising antigen presenting platform to activate NK cells. By enhancing the expression level of hallmark receptors, and increasing the secretion of cytotoxic factors, this may may synergistically intensify the NK cell-mediated cytotoxicity. NK-cells activated by antigens presented on the surface of CMNPs demonstrated significant killing effects on hepatoma cells and melanoma cells, therefore, CMNPs can be an important future toolkit towards clinical translation, supplementting adoptive cancer immunotherapy.

In the future work, it is worthwhile exploring the application of our platform in an autologous context, to potentially enhance clinical outcomes. As the number of immune cells with tumor-specific killing effects needs to be significantly expanded *in vitro* for clinical cancer immunotherapy, our easily tunable platform can facilitate the activation of NK cells and potentiate NK cells to a greater extent. In addition, previously employed strategies, such as the transitory activation of NK cells free, solution-bound agonists and cytokines, lead to low *ex vivo* expansion efficiency, whereas our platform is suitable for longterm proliferation. In this regard, the ability to easily separate nanoparticles from the NK cells presents a notable advantage. Furthermore, it is important to explore combined applications with other immunotherapeutic approaches such as immune checkpoint blockade and/or monoclonal antibody treatment, to

potentiate NK cell responses and to improve therapeutic effects against the barrier of immunosuppressive tumor microenvironments. Overall, tumor-antigen presenting biomimetic nanoparticles can potentially allow for enhanced NK cell-mediated cancer immunotherapy, which may yield promising clinical outcomes for cancer patients.

Author contributions

Dan Wu: Conceptualization, Methodology, Data curation, Formal analysis, Writing-original draft, Writing-review & editing. **Xin Shou:** Conceptualization, Methodology, Data curation, Formal Analysis. **Yalan Zhang:** Methodology. **Zihan Li, Guohua Wu, Di Wu, Jianguo Wu, Shengyu Shi:** Writing-review & editing. **Shuqi Wang:** Conceptualization, Project administration, Writing-review & editing, Supervision, Funding acquisition.

References

1. C. A. Klebanoff, S. A. Rosenberg and N. P. Restifo, Prospects for gene-engineered T cell immunotherapy for solid cancers. *Nat. Med.* 2016;22:26-36
2. S. A. Rosenberg and N. P. Restifo, Adoptive cell transfer as personalized immunotherapy for human cancer. *Science*. 2015;348:62-8
3. R. W. Wilkinson and A. J. Leishman, Further Advances in Cancer Immunotherapy: Going Beyond Checkpoint Blockade. *Front Immunol*. 2018;9:1082
4. I. Melero, A. M. Grimaldi, J. L. Perez-Gracia and P. A. Ascierto, Clinical development of immunostimulatory monoclonal antibodies and opportunities for combination. *Clin. Cancer. Res.* 2013;19:997-1008

5. N. W. van de Donk, P. Moreau, T. Plesner, A. Palumbo, F. Gay, J. P. Laubach, et al., Clinical efficacy and management of monoclonal antibodies targeting CD38 and SLAMF7 in multiple myeloma. *Blood*. 2016;127:681-95
6. V. Anagnostou, P. M. Forde, J. R. White, N. Niknafs, C. Hruban, J. Naidoo, et al., Dynamics of Tumor and Immune Responses during Immune Checkpoint Blockade in Non-Small Cell Lung Cancer. *Cancer Res.* 2019;79:1214-1225
7. L. Belcaid, S. Garaud, J. Kerger, S. Spyridon and S. Aspeslagh, Persistent anti-tumor response in cancer patients experiencing pneumonitis related to immune checkpoint blockade. *Acta Clin Belg*. 2019:1-5
8. E. Massarelli, W. William, F. Johnson, M. Kies, R. Ferrarotto, M. Guo, et al., Combining Immune Checkpoint Blockade and Tumor-Specific Vaccine for Patients With Incurable Human Papillomavirus 16-Related Cancer: A Phase 2 Clinical Trial. *JAMA Oncol*. 2019;5:67-73
9. D. Landi, M. Hegde and N. Ahmed, Human cytomegalovirus antigens in malignant gliomas as targets for adoptive cellular therapy. *Front Oncol*. 2014;4:338
10. D. A. Lee, Cellular therapy: Adoptive immunotherapy with expanded natural killer cells. *Immunol. Rev.* 2019;290:85-99
11. X. Ye, X. Liang, Q. Chen, Q. Miao, X. Chen, X. Zhang, et al., Surgical Tumor-Derived Personalized Photothermal Vaccine Formulation for Cancer Immunotherapy. *ACS Nano*. 2019;13:2956-2968
12. L. Zhang, W. Zhu, J. Li, X. Yang, Y. Ren, J. Niu, et al., Clinical outcome of immunotherapy with dendritic cell vaccine and cytokine-induced killer cell therapy in hepatobiliary and pancreatic cancer. *Mol Clin Oncol*. 2016;4:129-133

13. M. Daher and K. Rezvani, Next generation natural killer cells for cancer immunotherapy: the promise of genetic engineering. *Curr. Opin. Immunol.* 2018;51:146-153

14. J. I. Luna, S. K. Grossenbacher, W. J. Murphy and R. J. Canter, Targeting Cancer Stem Cells with Natural Killer Cell Immunotherapy. *Expert Opin Biol Ther*. 2017;17:313-324

15. K. B. Lupo and S. Matosevic, Natural Killer Cells as Allogeneic Effectors in Adoptive Cancer Immunotherapy. *Cancers (Basel)*. 2019;11

16. L. Zhu, S. Kalimuthu, P. Gangadaran, J. M. Oh, H. W. Lee, S. H. Baek, et al., Exosomes Derived From Natural Killer Cells Exert Therapeutic Effect in Melanoma. *Theranostics*. 2017;7:2732-2745

17. C. A. Alvarez-Breckenridge, J. Yu, R. Price, J. Wojton, J. Pradarelli, H. Mao, et al., NK cells impede glioblastoma virotherapy through NKp30 and NKp46 natural cytotoxicity receptors. *Nat. Med.* 2012;18:1827-34

18. V. Jelencic, M. Sestan, I. Kavazovic, M. Lenartic, S. Marinovic, T. D. Holmes, et al., NK cell receptor NKG2D sets activation threshold for the NCR1 receptor early in NK cell development. *Nat. Immunol.* 2018;19:1083-1092

19. D. Sanchez-Martinez, N. Allende-Vega, S. Orecchioni, G. Talarico, A. Cornillon, D. N. Vo, et al., Expansion of allogeneic NK cells with efficient antibody-dependent cell cytotoxicity against multiple tumors. *Theranostics*. 2018;8:3856-3869

20. C. Guillerey, N. D. Huntington and M. J. Smyth, Targeting natural killer cells in cancer immunotherapy. *Nat. Immunol.* 2016;17:1025-36

21. J. M. Kelly, P. K. Darcy, J. L. Markby, D. I. Godfrey, K. Takeda, H. Yagita, et al., Induction of tumor-specific T cell memory by NK cell-mediated tumor rejection. *Nat. Immunol.* 2002;3:83-90

22. H. Spits, J. H. Bernink and L. Lanier, NK cells and type 1 innate lymphoid cells: partners in host defense. *Nat. Immunol.* 2016;17:758-64

23. D. Wu, Y. Yu, C. Zhao, X. Shou, Y. Piao, X. Zhao, et al., NK-Cell-Encapsulated Porous Microspheres via Microfluidic Electrospray for Tumor Immunotherapy. *ACS Appl Mater Interfaces*. 2019;11:33716-33724

24. P. S. Becker, G. Suck, P. Nowakowska, E. Ullrich, E. Seifried, P. Bader, et al., Selection and expansion of natural killer cells for NK cell-based immunotherapy. *Cancer Immunol Immunother*. 2016;65:477-84

25. M. Granzin, A. Stojanovic, M. Miller, R. Childs, V. Huppert and A. Cerwenka, Highly efficient IL-21 and feeder cell-driven ex vivo expansion of human NK cells with therapeutic activity in a xenograft mouse model of melanoma. *Oncoimmunology*. 2016;5:e1219007

26. N. Sakamoto, T. Ishikawa, S. Kokura, T. Okayama, K. Oka, M. Ideno, et al., Phase I clinical trial of autologous NK cell therapy using novel expansion method in patients with advanced digestive cancer. *J Transl Med*. 2015;13:277

27. C. J. Denman, V. V. Senyukov, S. S. Somanchi, P. V. Phatarpekar, L. M. Kopp, J. L. Johnson, et al., Membrane bound IL-21 promotes sustained ex vivo proliferation of human natural killer cells. *PLoS One*. 2012;7:e30264

28. V. Balasubramanian, A. Correia, H. Zhang, F. Fontana, E. Makila, J. Salonen, et al., Biomimetic Engineering Using Cancer Cell Membranes for Designing Compartmentalized Nanoreactors with Organelle-Like Functions. *Adv Mater*. 2017;29

29. Y. Liu, J. S. Luo, X. J. Chen, W. Liu and T. K. Chen, Cell Membrane Coating Technology: A Promising Strategy for Biomedical Applications. *Nano-Micro Lett*. 2019;11

30. H. Q. Cao, Z. L. Dan, X. Y. He, Z. W. Zhang, H. J. Yu, Q. Yin, et al., Liposomes Coated with Isolated Macrophage Membrane Can Target Lung Metastasis of Breast Cancer. *Acs Nano*. 2016;10:7738-7748

31. R. H. Fang, C. M. J. Hu, B. T. Luk, W. W. Gao, J. A. Copp, Y. Y. Tai, et al., Cancer Cell Membrane-Coated Nanoparticles for Anticancer Vaccination and Drug Delivery. *Nano Lett.* 2014;14:2181-2188

32. R. H. Fang, A. V. Kroll, W. Gao and L. Zhang, Cell Membrane Coating Nanotechnology. *Adv Mater*. 2018;30:e1706759

33. R. Yang, J. Xu, L. Xu, X. Sun, Q. Chen, Y. Zhao, et al., Cancer Cell Membrane-Coated Adjuvant Nanoparticles with Mannose Modification for Effective Anticancer Vaccination. *ACS Nano*. 2018;12:5121-5129

34. R. H. Fang, A. V. Kroll and L. Zhang, Nanoparticle-Based Manipulation of Antigen-Presenting Cells for Cancer Immunotherapy. *Small*. 2015;11:5483-96

35. B. Furtmann, J. Tang, S. Kramer, T. Eickner, F. Luderer, G. Fricker, et al., Electrospray Synthesis of Poly(lactide-co-glycolide) Nanoparticles Encapsulating Peptides to Enhance Proliferation of Antigen-Specific CD8(+) T Cells. *J. Pharm. Sci.* 2017;106:3316-3327

36. J. Chi, C. Shao, Y. Zhang, D. Ni, T. Kong and Y. Zhao, Magnetically responsive colloidal crystals with angle-independent gradient structural colors in microfluidic droplet arrays. *Nanoscale*. 2019;11:12898-12904

37. A. V. Kroll, R. H. Fang and L. Zhang, Biointerfacing and Applications of Cell Membrane-Coated Nanoparticles. *Bioconjug Chem*. 2017;28:23-32

38. S. Bauer, V. Groh, J. Wu, A. Steinle, J. H. Phillips, L. L. Lanier, et al., Activation of NK cells and T cells by NKG2D, a receptor for stress-inducible MICA. *Science*. 1999;285:727-9

39. V. Groh, R. Rhinehart, H. Secrist, S. Bauer, K. H. Grabstein and T. Spies, Broad tumor-associated expression and recognition by tumor-derived gamma delta T cells of MICA and MICB. *Proc Natl Acad Sci U S A*. 1999;96:6879-84

40. E. Vivier, D. H. Raulet, A. Moretta, M. A. Caligiuri, L. Zitvogel, L. L. Lanier, et al., Innate or adaptive immunity? The example of natural killer cells. *Science*. 2011;331:44-9

Figures legends

Figure 1. Schematic depicting the synthesis of cancer cell membrane-coated nanoparticles (CMNPs) and their functions to stimulate NK cells for elevated tumor-killing responses.

Figure 2. Physicochemical characterization of CMNPs. (A) Transmission electron micrographs of (i) Fe_3O_4 nanoparticles, (ii) Fe_3O_4@SiO_2 nanoparticles and (iii) CMNPs. (B) Hydrodynamic sizes of Fe_3O_4, Fe_3O_4@SiO_2, CMNPs and cancer cell membrane vesicles analyzed by DLS. (C) Surface zeta potential of Fe_3O_4, Fe_3O_4@SiO_2, CMNPs and cancer cell membrane vesicles. The data were presented as mean ± SD (n = 3).

Figure 3. Characterization of membrane antigens on the surface of CMNPs. (A) Analysis of protein contents abundant in cancer cell cytosol, membranes and cancer cell membrane-coated CMNPs. All samples were analyzed on SDS-PAGE at the same protein concentration and subsequently dyed with a Coomassie Blue R250 solution. (B) Membrane-specific protein marker EGFR was detected by Western blotting. (C) Membrane-specific protein MICA/B was analyzed using flow cytometry.

Figure 4. Function characterization of activated NK cells stimulated by CMNPs. (A-C) The contents of IFN-γ, granzyme B and perforin by NK cells cocultured with CMNP at different membrane protein concentrations (*$p<0.05$, **$p<0.01$). (D) Flow cytometry analyses of the expression of surface activating receptors and markers on the non-stimulated NK cells and CMNPs-stimulated NK cells. Representative dot plots showed the activating receptor expression of NKG2D, NKp30, NKp44, NKp46, and CD69, respectively.

Figure 5. *In vitro* anti-tumor activity of CMNP-stimulated NK cells. Calcein-AM staining showed the survival of (A-B) HepG2 cells and (C-D) A375 cells incubated with CMNP-stimulated NK cells with E:T cell ratio of 5:1 of at 6 h or 12 h. Scale bar = 20 μm. Error bars indicate the mean ± SD (n = 3) (*p<0.05, ***p<0.001).

Figure 6. Killing effects of CMNP-stimulated NK cells on HepG2 and A375. Lactate dehydrogenase (LDH) release of (A) HepG2 cells and (B) A375 cells incubated with CMNPs stimulated NK cells at varying E:T cell ratios for 6 h or 12 h, respectively. The supernatant was collected, and the level of LDH was measured using a cytotoxicity LDH assay kit. Error bars indicate the mean ± SD (n = 3) (**p<0.01, ***p<0.001).

Graphical Abstract

Novel tumor cell-derived membrane coated Fe_3O_4@SiO_2 magnetic nanoparticles, containing tumor-specific antigens, serves an antigen presenting platform to activate NK cells by enhancing the expression level of surface activating receptors as well as markers (i.e., NKG2D, NKp30, NKp44, NKp46, and CD69), and increasing the secretion of cytotoxic factors including granzyme B, perforin and Active Ingredient-γ (IFN-γ) for enhanced NK cells-based immunotherapy.

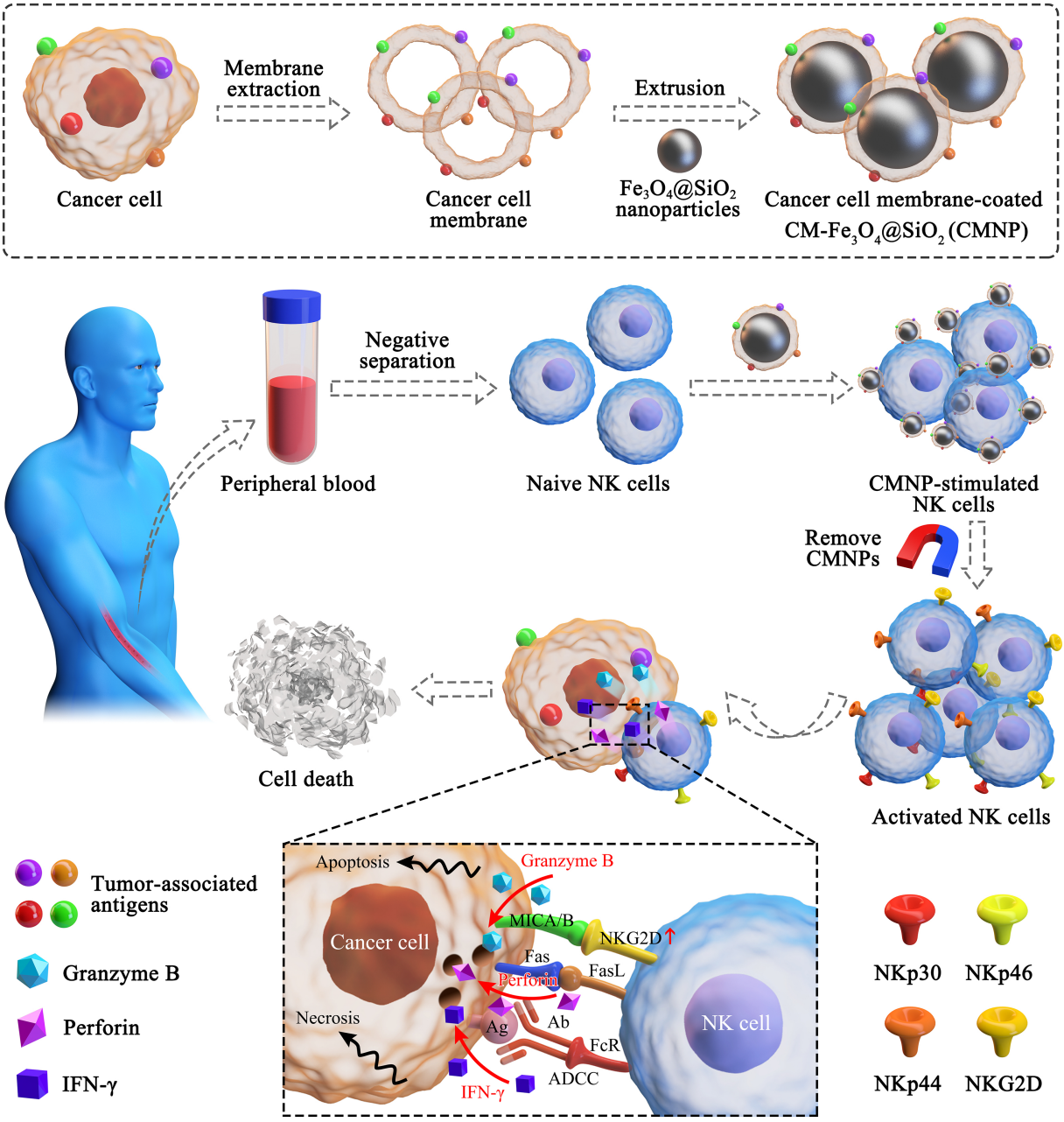
Cancer cell
Membrane extraction
Cancer cell membrane
Extrusion
Fe_3O_4@SiO_2 nanoparticles
Cancer cell membrane-coated
CM-Fe_3O_4@SiO_2 (CMNP)
Peripheral blood
Negative separation
Naive NK cells
CMNP-stimulated NK cells
Remove CMNPs
Activated NK cells
Cell death
Tumor-associated antigens
Granzyme B
Perforin
IFN-γ
Apoptosis
Granzyme B
Cancer cell
MICA/B
NKG2D
Fas
FasL
Perforin
Necrosis
Ag
Ab
FcR
ADCC
IFN-γ
NK cell
NKp30
NKp46
NKp44
NKG2D

Figure 1

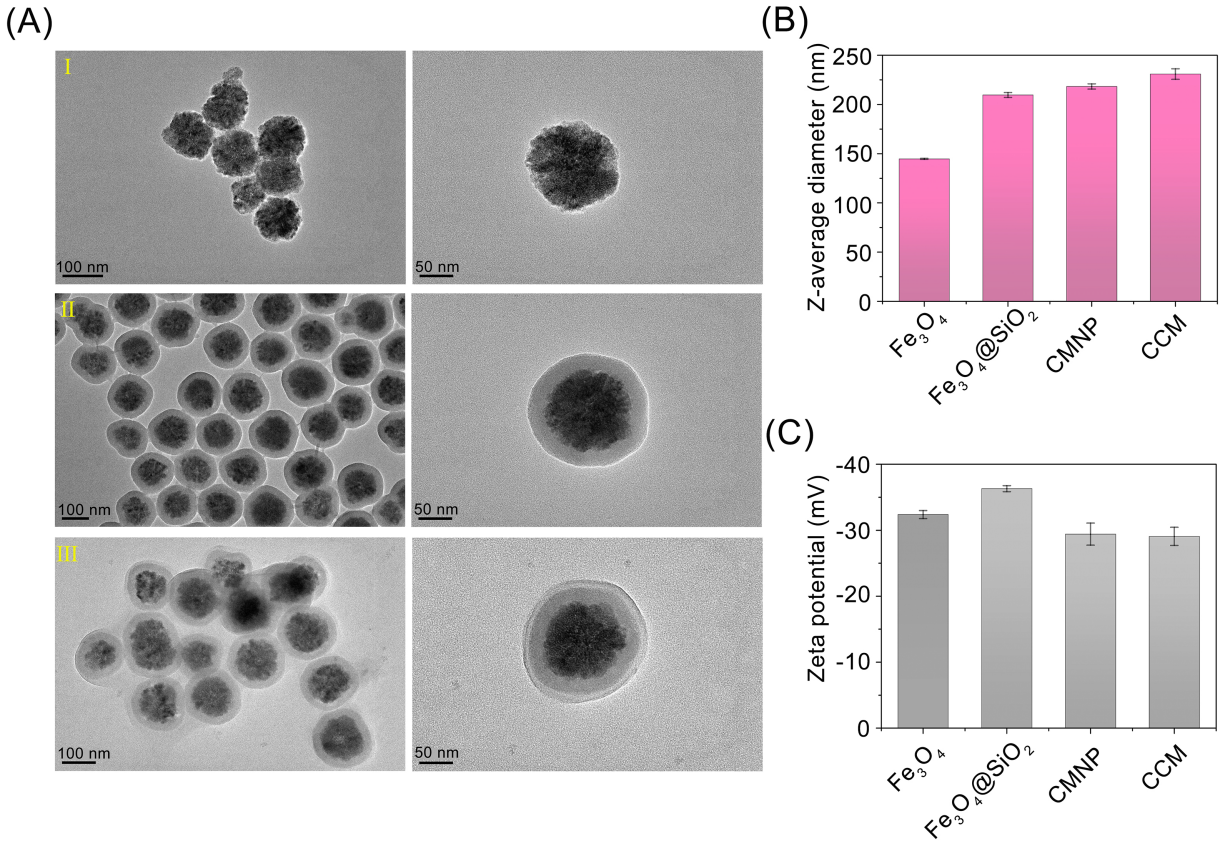
(A)
I
100 nm
50 nm
II
100 nm
50 nm
III
100 nm
50 nm
(B)
Z-average diameter (nm)
250
200
150
100
50
0
Fe3O4
Fe3O4@SiO2
CMNP
CCM
(C)
Zeta potential (mV)
-40
-30
-20
-10
0
Fe3O4
Fe3O4@SiO2
CMNP
CCM

Figure 2

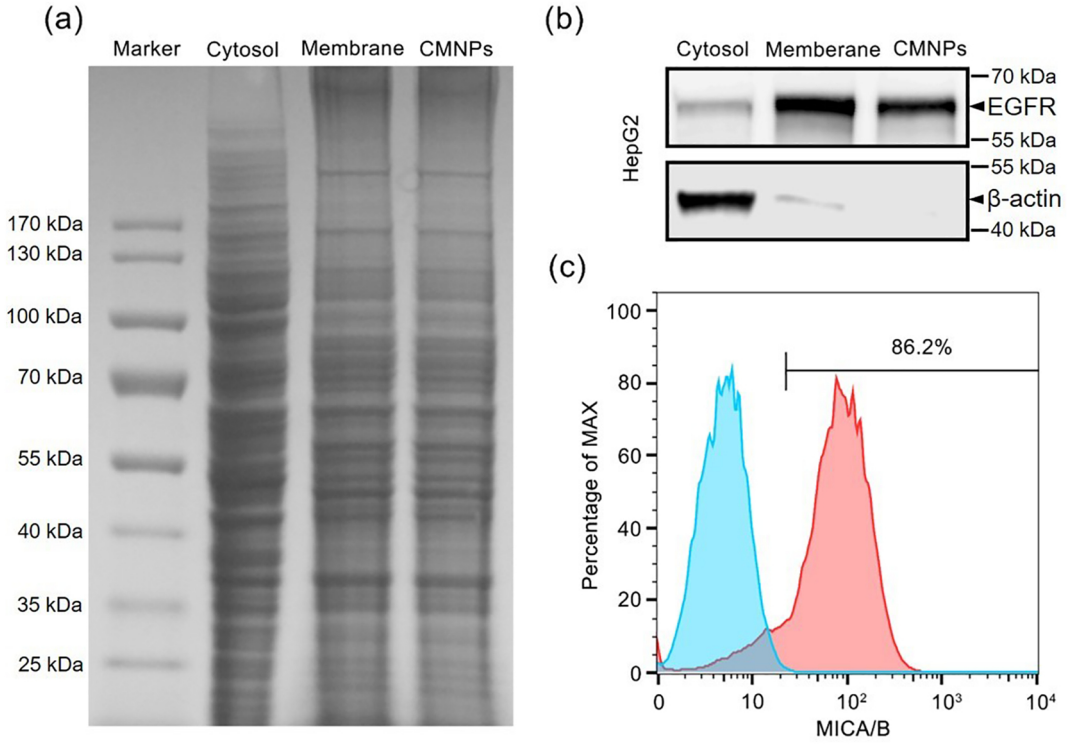
(a)
Marker
Cytosol
Membrane
CMNPs
170 kDa
130 kDa
100 kDa
70 kDa
55 kDa
40 kDa
35 kDa
25 kDa
(b)
Cytosol
Memberane
CMNPs
HepG2
70 kDa
EGFR
55 kDa
55 kDa
β-actin
40 kDa
(c)
86.2%
Percentage of MAX
MICA/B

Figure 3

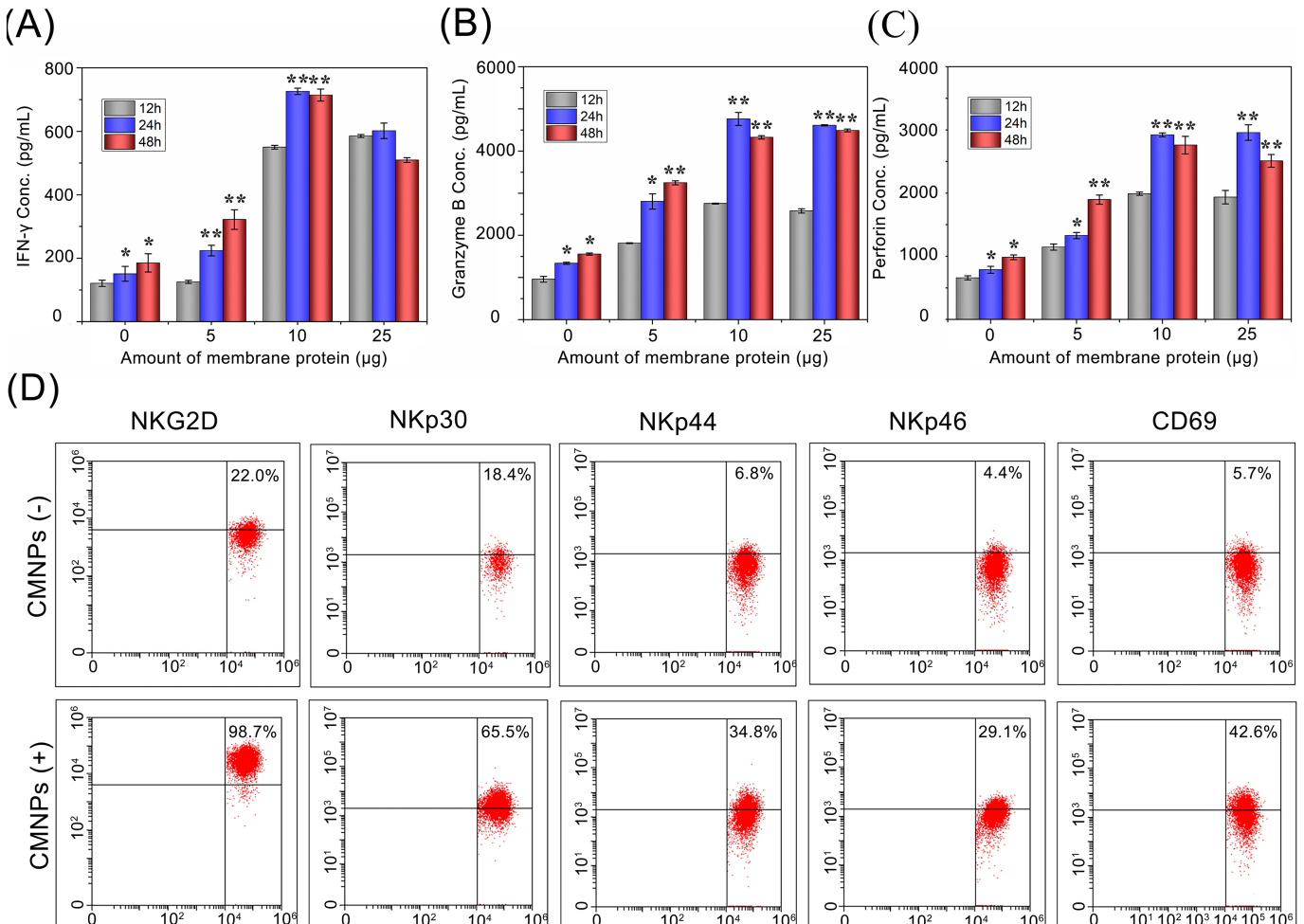
(A)
IFN-γ Conc. (pg/mL)
12h
24h
48h
Amount of membrane protein (μg)
(B)
Granzyme B Conc. (pg/mL)
12h
24h
48h
Amount of membrane protein (μg)
(C)
Perforin Conc. (pg/mL)
12h
24h
48h
Amount of membrane protein (μg)
(D)
NKG2D
NKp30
NKp44
NKp46
CD69
CMNPs (-)
22.0%
18.4%
6.8%
4.4%
5.7%
CMNPs (+)
98.7%
65.5%
34.8%
29.1%
42.6%

Figure 4

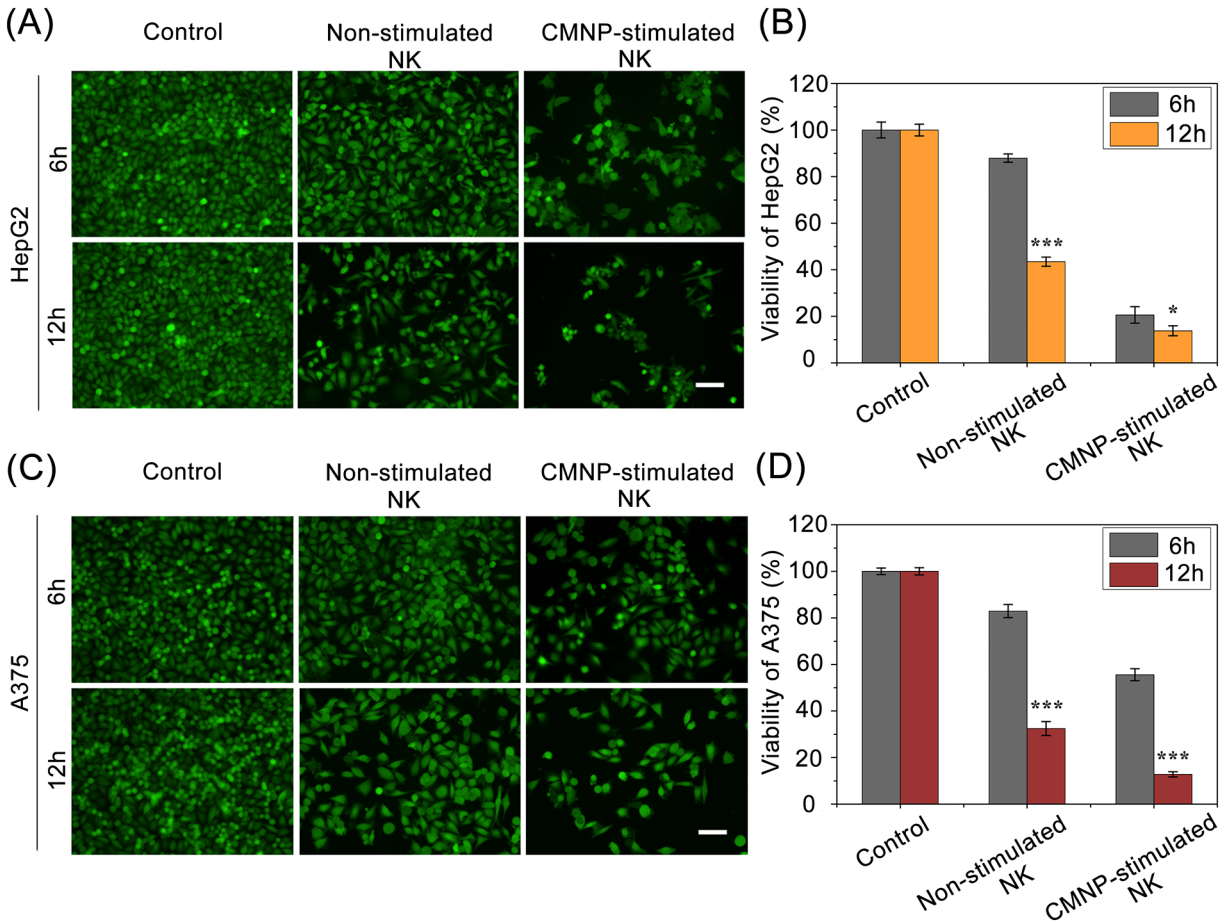
(A)
Control
Non-stimulated NK
CMNP-stimulated NK
HepG2
6h
12h
(B)
Viability of HepG2 (%)
6h
12h
***
*
Control
Non-stimulated NK
CMNP-stimulated NK
(C)
Control
Non-stimulated NK
CMNP-stimulated NK
A375
6h
12h
(D)
Viability of A375 (%)
6h
12h
***
***
Control
Non-stimulated NK
CMNP-stimulated NK

Figure 5

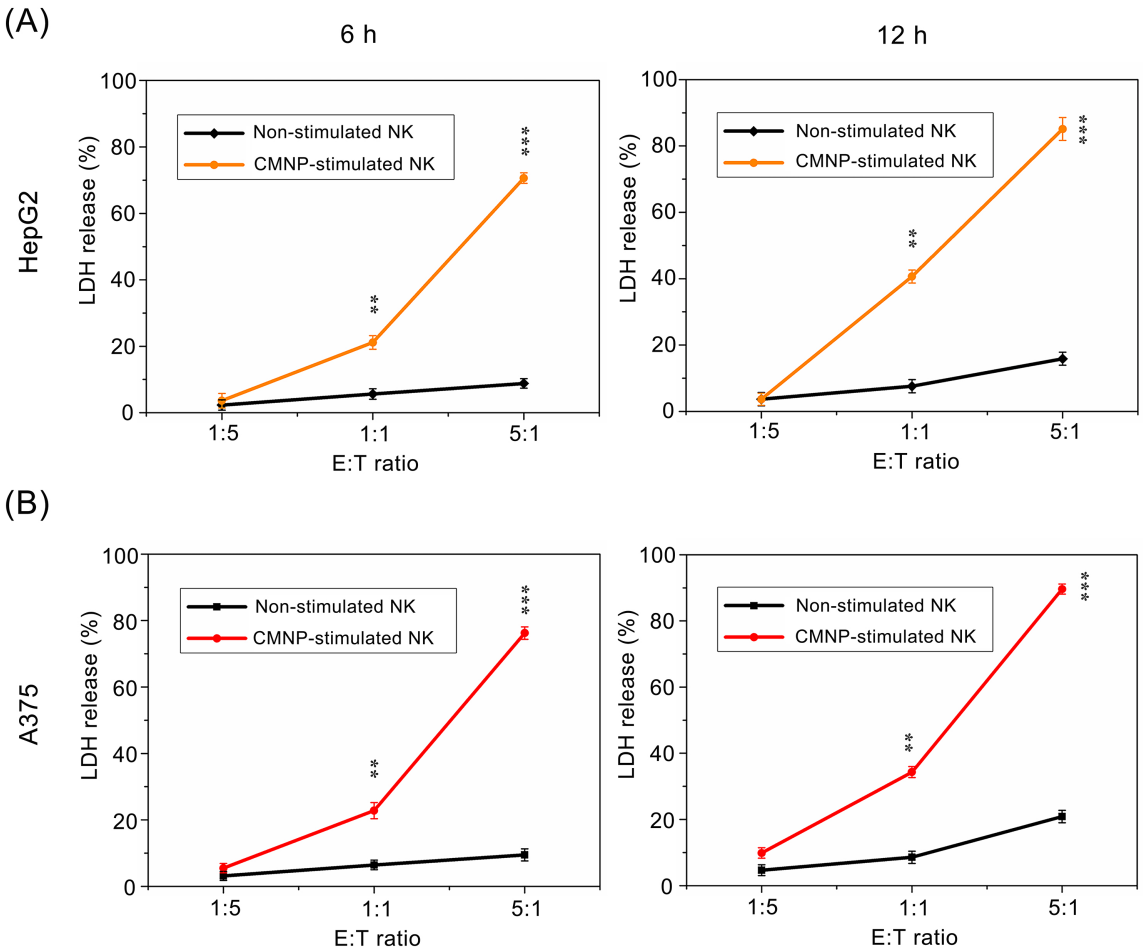
(A)
6 h
12 h
HepG2
LDH release (%)
Non-stimulated NK
CMNP-stimulated NK
**
***
1:5
1:1
5:1
E:T ratio
(B)
A375

Figure 6